Vaccine 39 (2021) 5302–5312

Contents lists available at ScienceDirect

Vaccine

journal homepage: www.elsevier.com/locate/vaccine

Optimal planning of the COVID-19 vaccine supply chain

Georgios P. Georgiadis, Michael C. Georgiadis *

Department of Chemical Engineering, Aristotle University of Thessaloniki, 54124 Thessaloniki, Greece

ARTICLE INFO

Article history:
Received 22 May 2021
Received in revised form 21 July 2021
Accepted 22 July 2021
Available online 27 July 2021

Keywords:
COVID-19
Vaccine supply chain
Optimal planning
MILP
Decomposition algorithm

ABSTRACT

This work presents a novel framework to simultaneously address the optimal planning of COVID-19 vaccine supply chains and the optimal planning of daily vaccinations in the available vaccination centres. A new mixed integer linear programming (MILP) model is developed to generate optimal decisions regarding the transferred quantities between locations, the inventory profiles of central hubs and vaccination centres and the daily vaccination plans in the vaccination centres of the supply chain network. Specific COVID-19 characteristics, such as special cold storage technologies, limited shelf-life of mRNA vaccines in refrigerated conditions and demanding vaccination targets under extreme time pressure, are aptly modelled. The goal of the model is the minimization of total costs, including storage and transportation costs, costs related to fleet and staff requirements, as well as, indirect costs imposed by wasted doses. A two-step decomposition strategy based on a divide-and-conquer and an aggregation approach is proposed for the solution of large-scale problems. The applicability and efficiency of the proposed optimization-based framework is illustrated on a study case that simulates the Greek nationwide vaccination program. Finally, a rolling horizon technique is employed to reactively deal with possible disturbances in the vaccination plans. The proposed mathematical framework facilitates the decision-making process in COVID-19 vaccine supply chains into minimizing the underlying costs and the number of doses lost. As a result, the efficiency of the distribution network is improved, thus assisting the mass vaccination campaigns against COVID-19.

1. Introduction

The unprecedented effects of SARS-COV-2 virus have risen an immense global interest regarding the development and distribution of safe and effective vaccines. Worldwide, more than 160 million people have been already infected, while close to 3.5 million passed away. In addition, the necessitated protective measures, and lengthy lockdowns have a severe financial impact on the society. The urge to rapidly decrease the toll of COVID-19 on health and global economy led to the rapid authorization of various vaccine candidates within a record time. While the focus in the vaccine world has been on developing the required vaccines and measuring their effectiveness, the struggle to understand and properly address the issues of the Vaccine Supply Chain (VSC) greatly reduces the impact of any vaccination program [1]. Mass vaccination of the world's population will achieve herd immunity, the first step for the progressive transition to the pre-COVID-19 normalcy. As a result, the biggest vaccination program in human history is currently in action pushing the COVID-19 VSC to its limits. Furthermore, special characteristics, like limited shelf-life and storage requirements in freezing conditions, makes its management a critical logistical challenge. Efficient and effective planning and operation of the supply chain is crucial for the success of the vaccination program, otherwise, numerous valuable doses will be wasted, and the program's progress will slow down, imposing important financial losses.

Few studies focus on VSCs, despite the substantial published research on supply chain optimization. Most related studies are concerned with problems related to the pharmaceutical sector [2–8]. More recent contributions address key problems of the pharmaceutical supply chain, like vehicle routing decisions [9,10], uncertainty [11], product perishability [12] and integrated capacity planning and scheduling [13], while few recent contributions focused on supply chains of CAR T-cell therapies [14–16]. Lately, the scientific community has shown an increasing interest in VSCs [17–19], especially on the design/redesign problem of VSC networks in developing countries [20–22]. Two extensive literature reviews on the topic of VSCs were recently published [23,24]. The optimal planning of the supply chain network has a strong positive effect on its efficiency. Therefore, a plethora of mathematical programming models have been proposed to address this

* Corresponding author.
E-mail address: mgeorg@auth.gr (M.C. Georgiadis).

https://doi.org/10.1016/j.vaccine.2021.07.068
0264-410X/

Nomenclature

Indices

i,j	Locations (manufacturing plants-hubs-vaccination centres)
v	Vaccine
c	Cold storage technology
t	Time periods
w	weeks

Sets

f_i	Manufacturing plants
h_i	Hubs
vc_i	Vaccination centres
cl_i	Clusters
FV	Vaccine v produced in manufacturing plant f
IJ	Connectivity between the locations of the supply chain
HVC	Connectivity between hubs h and vaccination centres vc
CV	Cold storage technology c necessary for long term storage of vaccine v
SL_v	Subset of vaccines that have a shelf-life smaller than the considered horizon

Parameters

$\pi^{max}_{h,v}$	Maximum supply of vaccine v to hub h *(vials)*
$\alpha_{i,v}$	Initial stored amount of vaccine v in location i *(vials)*
β_i	Ratio of vaccine wasted in location i
$\gamma_{h,c}$	Storage capacity of technology c in hub h *(vials)*
θ_{vc}	Storage capacity in vaccination centre vc *(vials)*
$\varepsilon_{i,v}$	Safety stock of vaccine v in location i *(vials)*
$\rho^{min}_{i,j}$	Minimum flow allowed between locations i and j
$\rho^{max}_{i,j}$	Maximum flow allowed between locations i and j
δ_v	Doses per vial of vaccine v
λ_v	Shelf-life of vaccine v in refrigeration *(days)*. Only relevant for vaccines with a shelf-life smaller than the considered horizon.
ζ_{vc}	Vaccination appointments goal for each vc
η	Number of vaccinations done daily by a vaccination line (Two healthcare workers)
ι_{vc}	Base number of healthcare workers in vaccination centre vc
ψ_c	Operating cost of cold storage technology c *(€ per daily storage of a single vial)*
κ	Average fuel consumption of truck transporting vaccines *(litres/100 km)*
φ	Fuel price *(€/litre)*
$\mu_{i,j}$	Distance between locations i and j *(km)*
τ	Average speed of vehicles transferring the vaccines
o	Cost of employing a driver *(€/hour)*
ξ_v	Cost of vaccine v *(€/dose)*
σ	Cost for utilizing extra healthcare workers (daily)
ν	Cost of renting a truck (Two weeks)

Variables

$X_{i,j,v,t}$	Amount of vaccine v transferred from location i to j in period t *(vials)*
$S_{i,v,t}$	Amount of vaccine v stored in location i in period t *(vials)*
$P_{f,v,t}$	Amount of vaccine v supplied by manufacturing plant f in t *(vials)*
$LS_{i,v,t}$	Wasted vials of vaccine v in location i in time period t
$VU_{vc,v,t}$	Vials of vaccine v used in vc in period t
$L_{vc,v,t,t'}$	Amount of vaccine v transferred in vc in t and used in t' *(vials)*
$WD_{vc,v,t}$	Wasted doses of vaccine v in vaccination centre vc in period t
$DU_{vc,v,t}$	Doses of vaccine v used in vc in period t
$DA_{vc,t}$	Vaccination appointments in location i in time period t
$VA_{i,v,t}$	Appointments using vaccine v in location i in time period t
$WE_{i,t}$	Vials wasted due to expiration in location i in time period t
WE^I_i	Vials from initial storage wasted due to expiration in location i in time period t
$HW_{i,t}$	Number of healthcare workers required in location in location i in time period t
$AH_{i,t}$	Additional healthcare workers (more than base) required in location i in time period t
NT	Number of trucks required for transportation
$SU_{vc,slv,t}$	Vials of initially stored vaccine slv used in vaccination centre vc in period t
$VU^I_{vc,v,t}$	Integer number of vials of vaccine v used in period t
$Y_{i,j,t}$	Binary variable that equals 1 if vaccines are transferred between locations i and j in period t

problem [25–27]. Despite the rich literature, only a handful of contributions consider the optimal planning of VSCs. Chen et al. developed the first planning model for a World Health Organization's Expanded Program on Immunization (WHO-EPI) distribution chain in developing countries [28]. Another study proposed a multi-objective, multi-period Mixed-Integer Linear Programming (MILP) model to address the simultaneous optimal design and planning of sustainable VSCs [29]. Trade-offs between the sustainability dimensions considered (economic, environmental, and social) are highlighted. Recently, Yang investigated the optimal design and operation of WHO-EPI vaccine distribution chains [30]. The author developed an MILP model and a disaggregation-merging technique to generate optimal solutions for real-world cases. Recently, Kontoravdi et al. presented a thoughtful discussion on the production phase of the vaccine [31]. The distribution phase of the COVID-19 supply chain has not been studied so far. A few contributions focus on the effect of the COVID-19 pandemic on other distribution supply chains [32]. The COVID-19 distribution chain displays special characteristics that differentiate them from other VSCs. A prominent concern regarding the distribution of COVID-19 vaccines is the strict temperature requirements during transportation and storage. Inefficient planning can lead to losses of many valuable doses and thus to increased operational costs. These negative implications are further amplified due to the enormous scale of the COVID-19 vaccination programs.

In this work, a new MILP model is presented for the optimal short-term planning of the COVID-19 supply chain network. Tactical and operational decisions regarding the inventory levels in the central hubs and vaccination centres, the vaccine flows between the various locations of the distribution network, the fleet requirements, the scheduling of citizens' vaccinations, as well as, staffing of the vaccination centres are simultaneously considered. The goal of the optimization is the minimization of cost. While previous works have addressed the medium-term VSC planning problem, the developed model is the first to consider key issues of the COVID-19 supply chain, like storage and supply limitations,

multiple cold storage technologies, demanding vaccination targets, transportation lead-times and vaccine perishability. Moreover, the literature models focus on economic or social objectives and do not take into account the minimization of wasted doses, a critical target for the effectiveness of the COVID-19 vaccination program. In addition to considering the minimization of dose wastage, the developed model is the first to simultaneously take optimal short-term decisions for the VSC and planning decisions for the vaccination program in each vaccination centre. Integrating these decisions enhances the efficiency of the overall vaccination program. An MILP-based solution strategy is introduced for the efficient solution of large-scale realistic case studies and is successfully applied to a case simulating the Greek COVID-19 VSC. Furthermore, a rolling-horizon technique is incorporated to replan the supply chain, in case of demand fluctuations originating from citizens that reschedule their vaccination appointment at the last minute or cancel a scheduled appointment. To the best of our knowledge this is one of the first contributions that examines the optimal planning of COVID-19 VSCs by integrating all key planning decisions for the efficient and cost effective realization of the citizens' vaccinations program.

2. Problem statement

The problem addressed in this work considers the optimal short-term planning of the COVID-19 VSC, as well as the optimal planning of appointments in the vaccination centres, in order to minimize the total costs. Fig. 1 illustrates a generic representation of the underlying network. The supply chain consists of three echelons: the manufacturing plants with a known maximum production capacity, the hubs, where the vaccine vials are stored and the vaccination centres, where the citizens are vaccinated. The product (vaccines) flow is unidirectional, from the manufacturers to the hubs and finally to the vaccination centres. Reverse flows from the vaccination centres to the hubs are not allowed, while intralayer flows between the hubs or the vaccination centres are not considered. Finally, the vaccines are used in the vaccination program of the population. Planning of the appointments is considered simultaneously with the planning the distribution of the COVID-19 vaccines. The capacity of the vaccination centres varies according to the employed healthcare personnel. To properly consider the low shelf-life of sensitive vaccines (5 days), a 14-day horizon is considered. The problem is described in terms of an MILP model that relies on a daily discretization of the time horizon. Within the given horizon a specific number of completed appointments must be satisfied. The model distributes them throughout the available periods. As a result, optimal decisions regarding the daily appointments at each centre are generated, which impose the needs in healthcare personnel.

Four vaccines with different characteristics are studied. In particular, the vaccines of Astrazeneca (A), Johnson& Johnson (J), Moderna (M) and Pfizer (P) are considered. Extension to more types of vaccines is straightforward since no changes in the developed model are necessary. Rather only an update on the set of vaccines v and all associated data, e.g. storage conditions, shelf-life etc. is required. The hubs are equipped with all necessary cold storage technologies for the long-term storage of the vaccines. More specifically, deep freezers (−70 °C) are required for Pfizer and regular freezers (−20 °C) for Moderna vaccines, while simple refrigeration suffices for the non-mRNA alternatives (A and J). In contrast, the vaccination centres are only equipped with regular refrigerators. This reinforces the need for the proper organization of the supply chain, since mRNA vaccines, especially the Pfizer vaccine, cannot be maintained long-term in refrigerated conditions. Therefore, perishability considerations are included in the proposed MILP model. A homogeneous fleet of trucks is employed to transport the vaccines from the hubs to the vaccination centres. The trucks are equipped with dry shippers to maintain low temperatures during transportation and ensure that the cold chain remains uninterrupted. Explicit truck capacity limits are not considered, they are matched by the vaccination centre's capacity. Vehicle routing is not considered in this study. It is assumed that in each period a truck can visit a single vaccination centre and must return to the hub from which it started. A daily lead-time is necessary for the transportation of vaccines between the echelons of the supply chain. An important issue in VSCs is related with the wasted doses. This is especially relevant for perishable products like the mRNA COVID-19 vaccines. The World Health Organization (WHO) categorizes the wasted doses into closed vial wastage, which is caused by inefficiencies in the supply chain and open vial wastage, which is further divided into avoidable and unavoidable open vial wastage [33]. The first is attributed to immunization workers and include errors in patients' reactions, suspected contamination, reconstitution, and excess heat. The latter refers to the discarded doses from multidose vials. Closed vial wastage and avoidable vial wastage are included in the model based on the wastage ratios recommended by WHO, while the minimization of the unavoidable open vial wastage is included in the objective function of the proposed model.

The objective of the proposed framework is to determine a) the transferred amounts and inventory profiles in each location, b) the daily vaccination appointments and the doses wasted due to open vials that are not fully exploited or due to expiration and c) the needs in healthcare personnel and fleet size to realize the vaccination program, so that the total cost of the supply chain is minimized. A cost term considers the valuable doses being wasted, while a backlog term is not included, since failing to realize a scheduled appointment is not allowed. Finally, the proposed framework examines a mature COVID-19 VSC, where vaccine availability issues have been overcome.

3. Mathematical framework

In this chapter the MILP-based mathematical frameworks that have been developed to deal with the optimization problem of planning the COVID-19 VSC are presented.

3.1. MILP model

The proposed model utilizes a discrete time grid to efficiently capture the inventory balances in the various locations of the supply chain. The constraints related to the material balances,

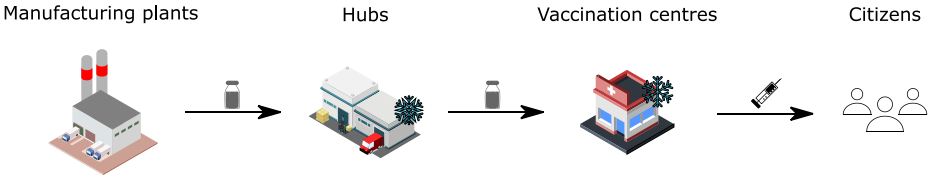

Fig. 1. Covid-19 Vaccine Supply Chain Representation.

inventory capacities and vaccine flows are inspired by the model proposed by Carvalho et al. [29]. In addition to the material balance, inventory capacity and flow limitation constraints, the proposed model introduces efficient constraints for the incorporation of lead-time, shelf-life limitations and the vaccination plan.

The supply limitations provided by the manufacturer are expressed by constraints (1) and (2). More specifically, constraints (1) ensure that the vials of vaccine v supplied by the corresponding manufacturer f ($P_{f,v,t}$) throughout the considered planning horizon are limited by the upper bound of production ($\pi^{max}_{h,v}$). Furthermore, it is assumed that each manufacturer f can supply each hub h at most once per week, as imposed by constraints (2). Constraints (3)–(7) encapsulate the material balances around each location of the supply chain. Firstly, constraints (3) guarantee that the amount of a vaccine v transferred from a factory f to all hubs h ($X_{f,h,v,t}$) equals the total amount supplied by the factory in time period t. The next two constraints set the material balances around the hubs. Constraints (4) state that the inventory at the end of the first time period equals the initial inventory of the hub ($\alpha_{h,v}$) plus the amount transferred from the factories, minus the amount that has been sent to the vaccination centres ($X_{h,vc,v,t}$) and the number of vials lost ($LS_{h,v,t}$). For all next time periods, the constraints remain the same, but instead of using the initial inventory, the inventory of the previous period is used. Similarly, constraints (6) and (7) monitor the material balances around the vaccination centres. Constraints (8) calculate the vials of vaccine v lost in each location i and time period t. Constraints (9) impose a minimum safety stock at the end of the planning horizon ($\varepsilon_{i,v}$), which is required to ensure the future availability of vaccines in the hubs and the vaccination centres. The storage capacities of the various technologies in the hubs and the vaccination centres are respected by constraints (10) and (11) accordingly. The minimum ($\rho^{min}_{i,j}$) and maximum ($\rho^{max}_{i,j}$)vial flows between locations are incorporated with constraints (12) and (13). Notice that when a connection is not realized in time period t ($Y_{i,j,t} = 0$), the associated transferred quantities ($X_{i,j,v,t}$) are zero.

At this point we should note, that while many variables are associated with an integer number of vaccines, e.g. $X_{f,h,v,t}$, $S_{h,v,t}$ etc., they are modelled as continuous variables. This is done to allow the prompt generation of optimal decisions. Modelling these variables as integer would result to a computationally intractable model even for medium-sized problem instances. To generate integer decisions, one could manually round the non-integer solution extracted by the model. Alternatively, the generated non-integer solution can be used as an initial solution for the same model, but with these variables defined as integer.

$$\sum_{f\in FV}\sum_{t} P_{f,v,t} \leqslant \pi^{max}_{h,v}\ \forall h, v \tag{1}$$

$$\sum_{t\in TW} Y_{f,h,t} \leqslant 1 \quad \forall f, h, w \tag{2}$$

$$\sum_{h} X_{f,h,v,t} = P_{f,v,t} \quad \forall f \in f v, v, t \tag{3}$$

$$S_{h,v,t} = \alpha_{h,v} + \sum_{f} X_{f,h,v,t} - \sum_{vc\in HVC} X_{h,vc,v,t} - LS_{h,v,t} \quad \forall h, v, t = 1 \tag{4}$$

$$S_{h,v,t} = S_{h,v,t-1} + \sum_{f\in FV} X_{f,h,v,t} - \sum_{vc\in HVC} X_{h,vc,v,t} - LS_{h,v,t} \quad \forall h, v, t > 1 \tag{5}$$

$$S_{vc,v,t} = \alpha_{vc,v} + \sum_{h\in HVC} X_{h,vc,v,t} - VU_{vc,v,t} - LS_{vc,v,t} \quad \forall vc, v, t = 1 \tag{6}$$

$$S_{vc,v,t} = S_{vc,v,t-1} + \sum_{h\in HVC} X_{h,vc,v,t} - VU_{vc,v,t} - LS_{vc,v,t} \quad \forall vc, v, t > 1 \tag{7}$$

$$LS_{i,v,t} = S_{i,v,t} \cdot \rho_i \quad \forall i, v, t \tag{8}$$

$$\sum_{v} S_{i,v,t} \geqslant \sum_{v} \varepsilon_{i,v}\ \forall i \in (vc_i \cup h_i), t = |T| \tag{9}$$

$$\sum_{v\in CV} S_{h,v,t} \leqslant \gamma_{c,h}\ \forall h, c, t \tag{10}$$

$$\sum_{v} S_{vc,v,t} \leqslant \theta_{vc} \forall vc, t \tag{11}$$

$$\rho^{min}_{f,h} \cdot Y_{h,vc,t} \leqslant \sum_{v\in FV} X_{f,h,v,t} \leqslant \rho^{max}_{f,h} \cdot Y_{h,vc,t}\ \forall f, h, t \tag{12}$$

$$\rho^{min}_{h,vc} \cdot Y_{h,vc,t} \leqslant \sum_{v} X_{h,vc,v,t} \leqslant \rho^{max}_{h,vc} \cdot Y_{h,vc,t}\ \forall h \in HVC, vc, t \tag{13}$$

An important characteristic of the studied supply chain concerns the required transportation time between the supply chain nodes. Theoretically, within the same day a vial could be transferred from the manufacturers to the hubs and then the vaccination centres to be used. However, this would require a finer discretization of time, thus resulting in large and computationally intractable models. Therefore, to ensure the feasibility of the proposed logistics operations using a daily discretization, it is assumed that a vial that is transferred from a manufacturing plant to a hub in period t, can only be further transferred to a vaccination centre after the next period ($t + 1$). The same holds for the hubs to vaccination centres connections. So, a transportation lead-time of one time period is included in the proposed model. These considerations are introduced to the model through constraints (14) and (15). Fig. 2 illustrates the role of the constraint for the vaccination centres. More specifically, the vials of vaccine v used in the vaccination plan in a vaccination centre for all periods $t' \leqslant t$, have to be less than or equal to the initial inventory plus the vials that arrived from the hubs in all periods $t'' \leqslant t - 1$, minus the vials lost in the same periods.

$$\sum_{vc}\sum_{t'\leqslant t} X_{h,vc,v,t'} \leqslant a_{h,v} + \sum_{f\in FV}\sum_{t''\leqslant t-1} X_{f,h,v,t''} - \sum_{t''\leqslant t-1} LS_{h,v,t''}\ \forall h, v, t \tag{14}$$

$$\sum_{t'\leqslant t} VU_{vc,v,t'} \leqslant a_{vc,v} + \sum_{h}\sum_{t''\leqslant t-1} X_{h,vc,v,t''} - \sum_{t''\leqslant t-1} LS_{vc,v,t''}\ \forall h, v, t \tag{15}$$

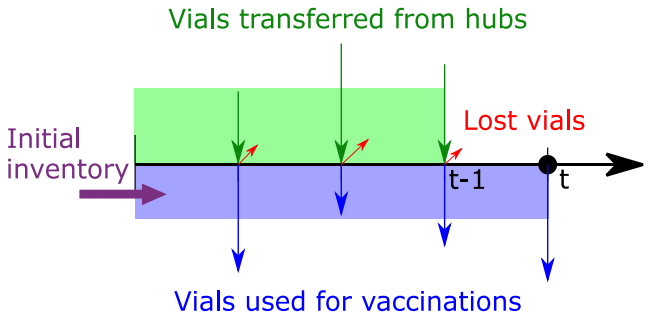

Fig. 2. Description of transportation time constraints.

To incorporate shelf-life issues in the model, a new variable $L_{vc,v,t,t'}$ is introduced, which defines the quantity of vials of vaccines v used in vaccination centre vc in time period t' that have been transferred to the vaccination centre in time period t. Constraints (16) state that the vials transferred to a vaccination centre in time period t are either used in the vaccination plan of the next time periods within the shelf-life of the specific vaccine (λ_{sl}) or are spoiled $WE_{vc,t}$. In case the time periods after t exceed the considered horizon, constraints (17) are activated to ensure that the vials used do not surpass the vials transferred. Another continuous variable is included to model the quantity of vials that existed in the initial inventory and were used in the vaccination plan of time period t ($SU_{vc,v,t}$). The next constraints connect the total quantity of vials used in the vaccination plan of period t ($VU_{vc,v,t}$), with the newly introduced variables. Finally, constraints (20) calculate the number of vials that belong in the initial inventory and are spoiled ($WE^{I}_{vc,t}$).

$$\sum_{t'\geqslant t+1}^{t+\lambda_{sl}} L_{vc,v,t,t'} + WE_{vc,t} = \sum_{h\in HVC} X_{h,vc,v,t}\,\forall vc, v\in SL, t \leqslant (|T| - \lambda_{sl}) \tag{16}$$

$$\sum_{t'\geqslant t+1} L_{vc,v,t,t'} \leqslant \sum_{h\in HVC} X_{h,vc,v,t}\,\forall vc, v\in SL, t > (|T| - \lambda_{sl}) \tag{17}$$

$$VU_{vc,sl,t'} = SU_{vc,sl,t'} + \sum_{t\leqslant t'-1} L_{vc,sl,t,t'}\,\forall vc, sl, t' \leqslant \lambda_{sl} \tag{18}$$

$$VU_{vc,sl,t'} = \sum_{t\geqslant t'-\lambda_{sl}}^{t'-1} L_{vc,sl,t,t'}\,\forall vc, sl, t' > \lambda_{sl} \tag{19}$$

$$\sum_{t\leqslant\lambda_{sl}} SU_{vc,sl,t} + WE^{I}_{vc} = \alpha_{vc,sl}\,\forall vc, sl \tag{20}$$

The daily vaccination appointments in vaccination centre vc and period t ($DA_{vc,t}$) are calculated as the summation of the doses of all vaccines v used in the respective vaccination centre ($DU_{vc,v,t}$), as shown in constraints (21). Constraints (22) define the number of vaccine doses as the product of the vials used and the number of doses in each vial. Attaining the vaccination target within the planning horizon is ensured by constraints (23).

$$\sum_{v} DU_{vc,v,t} = DA_{vc,t}\,\forall vc, t \tag{21}$$

$$VU_{vc,v,t}\cdot\delta_{v} = DU_{vc,v,t}\,\forall vc, v, t \tag{22}$$

$$\sum_{t} DA_{vc,t} = \zeta_{vc}\,\forall vc \tag{23}$$

Constraints (24) and (25) define the requirements in healthcare personnel for the vaccination plan. The number of daily appointments in a vaccination centre is dependent on the number of active vaccination lines in the centre ($HW_{vc,t}$). Based on the Greek COVID-19 vaccination program, it is assumed that each vaccination line consists of two health workers, that can complete η vaccinations per period. For each vaccination appointment a total of 15 min of registration and monitoring time is necessary, while each vaccination line is active for 6 h. Thus, parameter η takes the value 24 (6 h*4 appointments/h) in this study. However, the capacity of the vaccination centre is not limited by this value, since each vaccination centre comprises of multiple vaccination lines. More specifically, every vaccination centre has a base number of vaccination lines available (ι_{vc}) and an additional number of vaccination lines ($AH_{vc,t}$) can be activated to ensure the feasibility of the optimal vaccination plan. The fleet size required for distributing the vaccines from the hubs to the vaccination centres (NT) is calculated by constraints (26).

$$DA_{vc,t} \leqslant \eta\cdot HW_{vc,t}\,\forall vc, t \tag{24}$$

$$AH_{vc,t} \geqslant HW_{vc,t} - \iota_{vc}\,\forall vc, t \tag{25}$$

$$\sum_{h}\sum_{vc\in HVC} Y_{h,vc,t} \leqslant NT\,\forall vc, t \tag{26}$$

The vaccine doses wasted due to open vials that are not completely used within a period are included in the model using constraints (28). An integer variable is introduced to calculate the actual number of vials of vaccine v opened in vaccination centre vc and time period t ($VU^{I}_{vc,v,t}$), as shown in constraints (27). Finally, the doses available in the opened vials are subtracted by the actual doses used in the vaccination plan to calculate the number of wasted doses ($WD_{vc,v,t}$).

$$VU^{I}_{vc,v,t} \geqslant VU_{vc,v,t}\,\forall vc, v, t \tag{27}$$

$$WD_{vc,v,t} = (VU^{I}_{vc,v,t} - VU_{vc,v,t})\cdot\delta_{v}\,\forall vc, v, t \tag{28}$$

An economic objective that minimizes the total cost of the VSC, consisting of i) the storage costs, ii) the distribution costs (fuel consumption and drivers' wages), iii) the compensation for any additional healthcare personnel, iv) the wasted doses and v) the rental cost of the fleet, is considered (29).

$$\begin{aligned} min\ & \textstyle\sum_{h}\sum_{v}\sum_{c\in cs v_{c,v}}\sum_{t} S_{h,v,t}\cdot\kappa_{c} + \sum_{vc}\sum_{v}\sum_{t} S_{vc,v,t}\cdot\kappa_{refrigerator} \\ & + \textstyle\sum_{h}\sum_{vc\in HVC}\sum_{t} 2\cdot\mu_{h,vc}\cdot\left(\frac{\kappa\cdot\varphi}{100}\right)\cdot Y_{h,vc,t} + \sum_{h}\sum_{vc\in HVC}\sum_{t} 2\cdot\frac{\mu_{h,vc}}{\tau}\cdot o\cdot Y_{h,vc,t} \\ & + \textstyle\sum_{vc}\sum_{v}\sum_{t} WD_{vc,v,t}\cdot\xi_{v} + \sum_{vc} WE^{I}_{sl}\cdot\delta_{sl}\cdot\xi_{sl} + \sum_{vc}\sum_{t} WE_{sl,t}\cdot\delta_{sl}\cdot\xi_{sl} \\ & + \sigma\cdot\textstyle\sum_{vc}\sum_{t} AH_{vc,t} + \nu\cdot NT \end{aligned} \tag{29}$$

3.2. MILP-based solution strategy

For the solution of large problems, an MILP-based strategy, based on a decomposition algorithm is employed. Let us assume a relatively small problem with one manufacturing plant, two hubs and 20 vaccination centres. The problem is decomposed employing the following rationale. First, the problem is divided into two subproblems, one for each hub, where the vaccination centres are preallocated to the closest hub. This assumption is motivated by the observation that in large problems, the vaccination centres will never be supplied by the hubs that are far away from them. So, this approach does not strongly affect the quality of the solution, however, it reduces immensely the combinatorial complexity of the problem, since many binary variables (connections between hubs and vaccination centres) are predefined. Next, the vaccination centres are grouped into clusters based on existing political boundaries. As shown in Fig. 3, four clusters are generated, two for each subproblem. Then, the two subproblems are solved using the cluster entities, instead of the vaccination centres. To generate the models, all related parameters of the vaccination centres, e.g. vaccination targets, storage capacities etc. are aggregated to extract the parameters for each cluster. Through this aggregated approach, small problems that can be quickly solved are generated. The solution of these models proposes optimal decisions considering the clusters as the last echelon of the VSC. To disaggregate these decisions an additional step is introduced. Here, all binary variables are fixed, and the previous solution is used as a start point for the solver, meaning that in case hub h is supplying vaccines to cluster cl in time period t ($Y_{h,cl,t} = 1$), then at this time period the hub will supply all vaccination centres of this cluster. Since, no

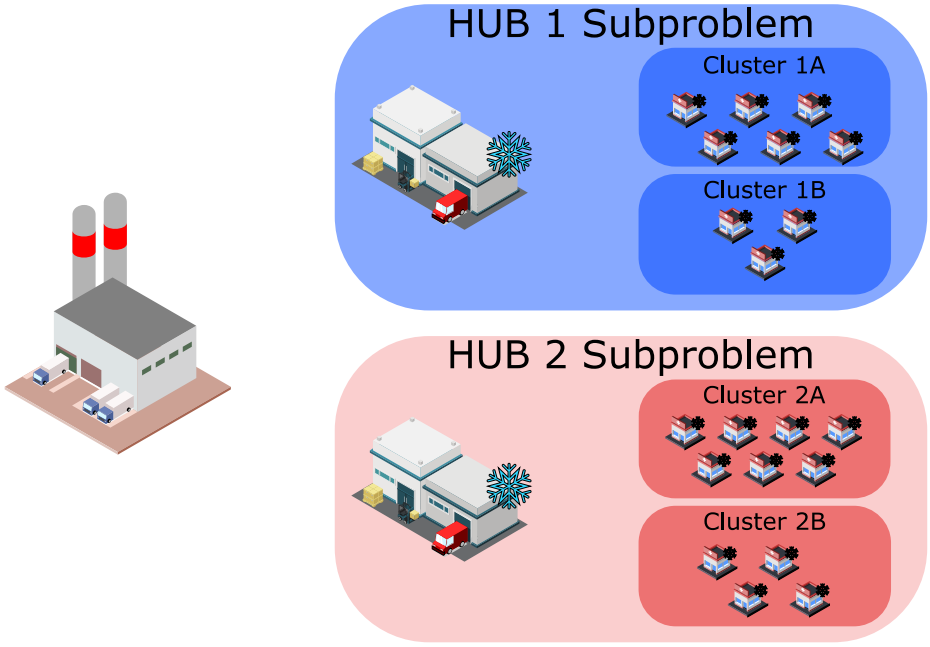

Fig. 3. Decomposition approach.

binary variables are optimized, the model is reduced to an LP model, so it can be solved very fast.

Conclusively, the proposed solution strategy consists of two steps. In the first step, small subproblems are generated, first through a divide-and-conquer approach that creates MILP-subproblems for each hub, and then by an aggregation technique that reduces the number of involved entities, by grouping the vaccination centres into clusters. At this point the reduced MILP-subproblems are solved to provide optimal solutions for the clusters. In the second step of the algorithm, the binary decisions are fixed, and an LP-model is now solved for all vaccination centres. Sequentially, the MILP-subproblems for each hub are solved and finally the optimal plan for the entirety of the supply chain is created.

3.3. MILP-based replanning algorithm

Often citizens do not arrive to the planned appointment or reschedule their appointment at the last minute. This is a known issue in COVID-19 VSCs that must be considered, otherwise the variations between the planned and the actual vaccinations, may result to suboptimal or even infeasible solutions. Possible consequences could be the spoilage of numerous doses, the failure of achieving the vaccination targets, the violation of inventory limitations or the miscalculation of the needs in healthcare personnel. Therefore, a reactive approach is employed, utilizing the MILP-based solution strategy in the context of a rolling horizon algorithm to ensure that the supply chain is properly replanned.

The introduction of four new subsets T_p, T_r, T_f and T_c is required for the implementation of the algorithm. T_p defines the prediction horizon, which includes all time periods considered by the optimization model at each iteration. In this study a bi-weekly prediction horizon is considered ($|T_p| = 14$). Fully reoptimizing the plan will provide the best possible solutions in terms of the underlying economic objective; however, it may require a significant number of changes, leading to nervousness, that could not be implemented in practice. Therefore, the prediction horizon subset is further divided into two subsets T_r and T_f. The first corresponds to the initial part of the prediction horizon, in which the decisions related to the binary variables ($Y_{i,j,t}$) and the daily number of vaccines used ($VU_{vc,v,t}$) remain fixed and equal to the previous solution. The second horizon is more flexible since the previous solution for the variables related to the connections between locations of the supply chain and the vaccines used is applied as a lower bound. This ensures that the scheduled appointments will not be rescheduled, however more appointments or additional connections are possible to improve the quality of the plan. The length of these horizons can be freely chosen by the decision-makers based on their specific goals. In this study, equally length horizons are used ($|T_r| = |T_f| = 7$), which achieve a good trade-off between nervousness and solution quality. The rest of the variables, e.g. inventory profiles, transferred quantities etc., are fully relaxed throughout the prediction horizon. Finally, T_c corresponds to the control horizon, that includes all time periods for which the optimized decisions are applied. Usually the control horizon is set to a minimal of one time period, which allows the re-optimization of the plan after every time period ($|T_c| = 1$). The initial state of the supply chain in a given prediction horizon $T_{p,h}$ equals to the final state of the previous control horizon $T_{c,h-1}$. At the end of each period the model receives the new information regarding the actual vaccination appointments and the new inventory levels at the vaccination centres.

Let us assume an illustrative example with the following horizon lengths, $|T_p| = 14$, $|T_r| = |T_f| = 7$ and $|T_c| = 1$, with initial time periods $\{t1, ..., t14\}$, $\{t1, ..., t7\}$, $\{t8, ..., t14\}$ and $\{t1\}$ accordingly. Initially the solution strategy computes the optimal plan for $|T_p|$. At this point the size of fleet is decided, which is the only decision variable that remains fixed. The plan will be implemented only for period $t1$. The information for the actual vaccinations done and the true levels of inventory in the vaccination centres becomes available at the end of the period. Then the horizon rolls and the subsets are updated so that $T_p = \{t2, ..., t15\}$ $T_r = \{t2, ..., t8\}$ and $T_f = \{t9, ..., t15\}$. Using the new information and the previous solution, the proposed optimization-based solution strategy is employed. This procedure continues iteratively until the finalization of the vaccination program. Fig. 4 illustrates the defined horizons for four consecutive iterations of the rolling horizon algorithm.

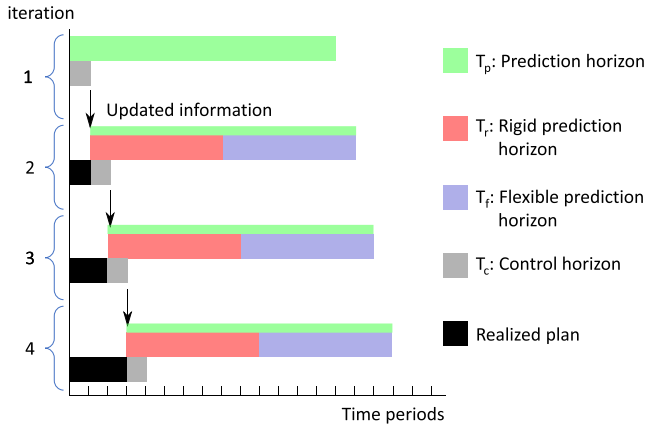

Fig. 4. Replanning via a rolling horizon approach.

The implementation of this algorithm incorporates uncertainties of the COVID-19 supply chain related to the differences between the planned and the actual appointments in the modelling approach. Thus, the decision-makers can deal with such uncertainties and constantly improve the extracted plans using the current state of the supply chain. Decisions related to transferred quantities, employed healthcare personnel and inventories can be promptly adjusted to include any new information, ensuring the success of the vaccination program, while minimizing the total operational costs.

4. Results

In this section the developed optimization-based framework is tested. First, an illustrative example is used to test in detail the efficiency of the proposed MILP-model. Then, a large-scale problem that simulates the Greek COVID-19 VSC is studied and near-optimal planning decisions are generated by employing the proposed MILP-based solution strategy. Finally, the applicability of the replanning algorithm is illustrated even for extreme disturbances in the vaccination plan. All models and solution algorithms were developed using the GAMS 30.1 interface and all instances were solved in an Intel Core i7 @3.4Gz with 16 GB RAM using the commercial solver CPLEX [34].

4.1. Illustrative example

Let us assume a COVID-19 supply chain consisting of one hub and five vaccination centres. Two vaccine types (P and M) are available, supplied by two manufacturing plants. Each plant is exclusively producing and supplying to the hubs only one vaccine type. All related data e.g. storage capacities, vaccination goals, distances etc. are provided in the supplementary material (Tables S1–S5). The Pfizer-type vaccine can be stored for up to 5 days in the vaccination centres, while perishability constraints are not enforced on the Moderna-type vaccine, whose shelf-life in refrigerated conditions (30 days) greatly exceeds the bi-weekly planning horizon.

The developed MILP model is employed to minimize the total cost for the distribution of the vaccines and the planning of the vaccination program in the vaccination centres. Within 30 CPU seconds, an optimal solution with a minimum cost of 22,059 RMUs[1] is generated. The most significant costs are associated with the operation of the storage technologies, especially the freezers and deep freezers in the hubs. In particular, 59.8% of the total costs originate from storing the vaccines in the hubs and 19.1% are due to storage costs in the refrigerators of the vaccination centres. Thus, inventory costs comprise the 78.9% of the total cost, emphasizing the importance of generating decisions that optimize the inventory profiles of the supply chain. Fuel costs, drivers' wages, and rental of the trucks, cover 3.8%, 9.3% and 6.1% of the total cost accordingly. Only 26 doses are lost translating to 1.8% of the total costs. No additional healthcare personnel are required; therefore, the associated cost term is zero. Table 1 reports the number of vaccine vials stored in the hub and the vaccination centres throughout the considered horizon ($S_{i,v,t}$). Further detailed results on the vials transferred ($X_{i,j,v,t}$), the vials opened ($VU^{I}_{i,v,t}$), the doses used ($DU_{i,v,t}$), the daily appointments ($DA_{i,t}$), the solution statistics and the cost distribution can be found in Tables S6–S11 of the supplementary material.

4.2. Large-scale study case: The Greek COVID-19 VSC

To evaluate the developed MILP-based framework for realistically sized COVID-19 VSCs, the problem of the panhellenic vaccination program is simulated. The Greek state is using five hubs in total, whose exact locations are unknown due to security reasons. However, it is known that two are in the region of Attica, one in Thessaloniki, one in Karditsa and one in Crete. Based on this knowledge the locations of the hubs are approximately chosen. The hospitals and health centres of Greece as provided by the Hellenic Ministry of Health are used as vaccination centres. Except for Crete, which has its own hub, Greek islands are not considered in the study. As a result, a total of 351 vaccination centres are considered. Four vaccine types are available (P, M, A, J) each one produced and supplied exclusively by a single manufacturing plant. To create the required data, the population data of Greece from the Population and Housing Census conducted by the Hellenic Statistical Authority are used [35]. The population is divided based on the regional unit and the vaccination centres are allocated to their respective regional unit. To generate the vaccination targets for the considered horizon of 14 days, it is assumed that the vaccination program for the entirety of the population must be realized within 6 months. So, the total demand for each vaccination centre is divided by 12 to get the bi-weekly vaccination targets. To ensure the feasibility of the problem, the initial inventory in the hubs and the vaccination centres is enough to satisfy at least the vaccination demand of the first two time periods. Vaccine inventories in the manufacturing plants are not considered as they are irrelevant for the problem under consideration.

The problem above is solved by employing the proposed MILP-based solution strategy. Each vaccination centre is allocated to a single hub based on the geographical criteria. For the aggregation step of the solution algorithm, the 351 vaccination centres are grouped into 54 clusters based on their regional unit. Detailed data of the considered problem instance e.g. maximum vaccine supply, distance matrix, hub to vaccination centres connectivity and vaccination centres to clusters allocation, are provided in Tables S12–S17 of the supplementary material. To generate near-optimal solutions for the entirety of the supply chain, five individual subproblems, one for each hub are solved. First the clusters are considered, and aggregate solutions are proposed and then the detailed solutions for all vaccination centres of the subproblems are generated. The solver terminates either when the computational time limit of one hour (3600 s) is exceeded, or when an optimality gap of 5% is achieved. Table 2 portrays the solution statistics for all iterations of the individual subproblems. It is shown that the computational time limit is reached for the more complicated cases (H1, H2 and H3) in the first step of the solution strategy. However, the optimality gaps achieved are very close to the desired target of 5%. This target has been chosen, since a solution with a proven optimality gap

[1] Relative Monetary Units

Table 1
Stored vials in the hub and in the vaccination centres ($S_{i,j,t}$).

		t1	t2	t3	t4	t5	t6	t7	t8	t9	t10	t11	t12	t13	t14
H	**P**	3	3				975	21	21	3	2	977	240	240	240
H	**M**		735						1234	269	242	242	242	242	242
C1	**P**	5	2	1				332	184	42	7	4	289	289	289
C1	**M**	177	89	254	166	77	6	6	3	333	264	175	87	87	87
C2	**P**	98	2	2	1	1	1	276	138	7	2	1	213	213	213
C2	**M**	105	80	244	161	79				320	238	155	74	74	74
C3	**P**	88		1				176	87	3			138	138	138
C3	**M**	51	50	157	103	50				207	154	100	47	47	47
C4	**P**	56	12	9	5	4		95	50	9	5	1	68	68	68
C4	**M**	23	22	72	47	20				99	73	48	23	23	23
C5	**P**	15						67	46	26	12		31	31	31
C5	**M**	56	53	40	27	15	3	3	3	2	25	20	8	8	8

Table 2
Solution statistics for the Greek Study Case.

	First step (Aggregate solution)					
	CPU	Variables	Binary Variables	Equations	Solution	Gap
H1	3600	18,993	986	12,269	283,808	7%
H2	3600	15,073	986	10,309	189,815	8%
H3	3600	13,421	738	8845	171,274	8%
H4	25	13,323	614	8477	384,564	<5%
H5	1365	4846	304	3441	65194.23	<5%
	Second step (Detailed solution)					
	CPU	Variables	Binary Variables	Equations	Solution	Gap
H1	158	47,391	5088	41,731	291,435	<1%
H2	71	32,446	3408	28,431	192,462	<1%
H3	25	32,425	3456	28,587	176,151	<1%
H4	13	35,190	3792	31,135	387,297	<1%
H5	1.6	10,718	1104	9575	66,164	<1%

of 5% can be considered as optimal. It must be noticed that for these cases relatively good optimality gaps (15–20%) were achieved in very low CPU times, of around 15 min, displaying the model's capability of quickly proposing good solutions for complex problems. On the contrary, subproblems H4 and H5 are promptly solved to optimality. The time required for the second step is very low in comparison. Even the most difficult subproblem (H1) is resolved within three minutes. Comparing the problem sizes of the first and second step it is observed that the aggregated approach significantly reduces the number of variables and equations, which makes feasible the consideration of large and complex problem instances. The computational time required in total is close to 3.5 h, however the utilization of parallel computing techniques reduces it to around 1 h. Optimal solutions are generated for the smaller subproblems, while larger, more difficult subproblems may not be solved to optimality, but the reported integrality gaps (<8%), signify a solution close to the optimal one (5%).

Fig. 5 displays the distribution of the various cost terms for the study case of Greece. Similar conclusions to the ones for the illustrative example can be drown. Storage costs in the hubs and the vaccination centres are the most significant terms, comprising together the 78% of the total costs. Next come the transportation costs, more specifically the wage of the drivers (9%), the cost of renting the trucks (8.4%) and the cost of fuel (3.8%). Finally, very few doses are lost (0.7%), while extra healthcare workers are rarely required (0.3%). The precise cost distribution for each of the five subproblems solved are provided in Table S18 of the supplementary material. Fig. 6 illustrates the inventory profiles in each of the hubs and aggregated for all vaccination centres. It is noticed that the stored amounts are sustained relatively low to reduce as much as possible the storage costs. This is especially evident for the Pfizer-type and Moderna-type vaccines, which consistently do not remain in storage, rather they are used as fast as possible. This is expected since the mRNA vaccines are stored using special technologies that impose high operational costs. The stored amounts are increased in the end of the horizon to satisfy safety stock requirements. Low quantities of Pfizer-type vaccine are observed in the inventory profiles of the vaccination centres which ensure that the vaccines are not spoiled due to perishability issues. Moreover, the inventories of the vaccination centres at the end of Saturdays (time periods 6 and 13) are practically zero since it is assumed that no vaccinations are done on Sundays.

In the presented example the vaccination centres have been grouped based on political boundaries. However, different clustering methods could be applied in other VSC problems. To address the impact the number of clusters employed have in the quality of the solutions generated, the following sensitivity analysis is included. Employing the proposed solution strategy, a large-sized problem of 106 vaccination centres is considered. A total of six instances are solved, considering alternative grouping of the vacci-

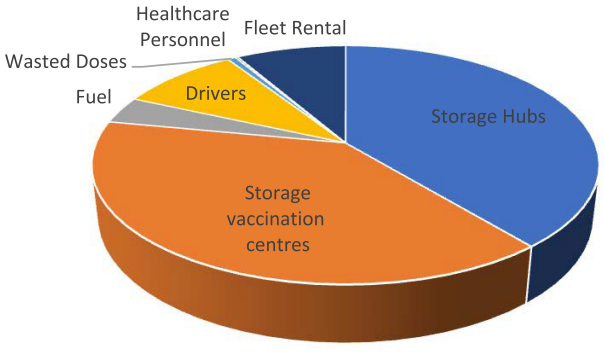

Fig. 5. Cost distribution.

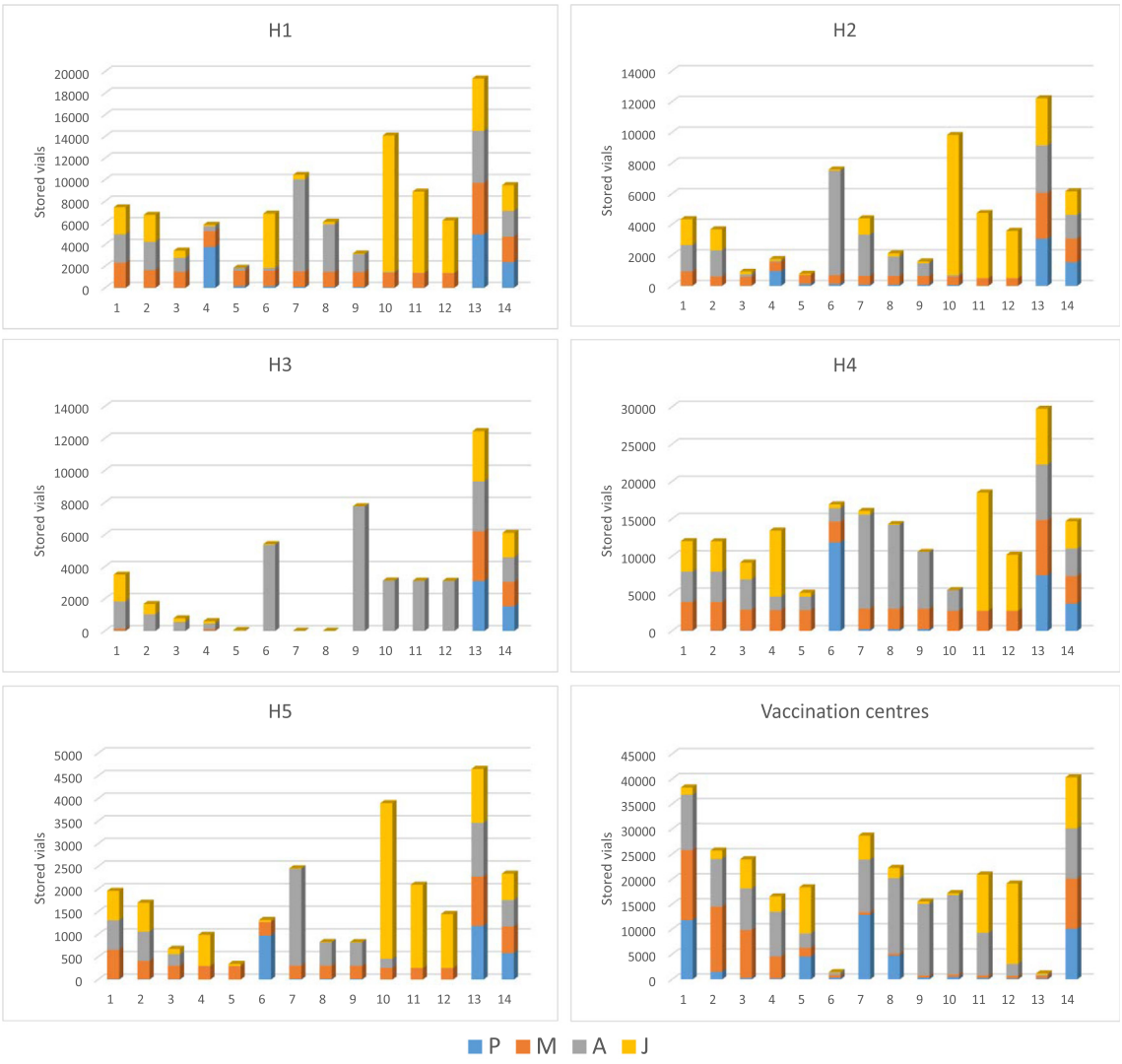

Fig. 6. Inventory profiles in hubs and vaccination centres.

nation centres into clusters. More specifically, 10–15 clusters are used in the studied instances. Table 3 summarizes the results of this analysis. As expected, using less clusters results to smaller MILP models in the first step. Therefore, the aggregated solution extracted is closer to the theoretically optimal, since smaller integrality gaps are achieved. However, aggregating the vaccination centres into fewer clusters, leads to worse solutions, when dealing with the real VSC problem. In particular, the generated LP model in the second step leads to worse detailed solutions for the vaccination centres. Interestingly, using 10 or 11 clusters in the studied example results to infeasibly solutions. Therefore, extremely aggregating the vaccination centres into very few clusters should be strongly avoided. Conclusively, the maximum number of clusters, that respects the comptutational time limitations, should be selected.

4.3. Replanning the COVID-19 VSC

In this subsection the problem of replanning the COVID-19 VSC in case of disturbances due to citizens not arriving to scheduled appointments is studied. The case study used replicates the subproblem of hub H1 from the Greek nationwide problem presented in the previous section. First, the model is solved for the initial 14-day horizon. At the end of the first period, the decision makers

Table 3
Impact of number of clusters employed on solution performance.

Clusters	N. Eq.	N. Var	N. BVar	CPU (s)	GAP (%)	Agg. Sol	Det. Sol
15	12,269	18,993	986	3600	9.6	186,425	188,686
14	11,889	18,552	924	3600	9.3	172,208	191,740
13	11,509	18,111	862	3600	9.2	173,220	193,130
12	11,129	17,670	800	3600	9.2	171,605	195,472
11	10,749	17,229	738	3600	8.8	153,935	NA
10	10,369	16,788	676	3600	8.5	143,221	NA

Table 4
Cost distribution for every iteration of the rolling horizon algorithm.

Iter	Storage Hubs	Storage Centres	Fuel	Drivers	Wasted Doses	Healthcare Personnel	Fleet Rental	Total
1	27,202	47,520	7548	18,580	846	954	21,330	123,981
2	22,703	44,329	6280	15,457	1337	1080	21,330	112,517
3	24,401	37,839	5442	13,395	803	1018	21,330	104,228
4	24,202	37,367	5676	13,971	791	1022	21,330	104,359

gather the following information. All scheduled appointments were completed in only 26 vaccination centres. In 15 of them 5% of the appointments were not realized, while 10% and 15% of the citizens did not arrive in the appointments in 44 and 21 vaccination centres accordingly. Similarly, in the second period, the percentage of unrealized appointments was 2% in 45, 8% in 11 and 12% in 30 vaccination centres, while on the third period these were 4% in 30, 10% in 40 and 25% in 6 vaccination centres. Those disturbances call for the immediate replanning of the supply chain since the actual inventory profiles are significantly different to the planned ones. Therefore, when the new information becomes available, the proposed solution strategy is employed to reactively replan the supply chain. The cost distribution after every iteration of the solution algorithm is shown in Table 4. It is observed that despite the significant disturbances, the costs remain low. Interestingly, very few doses are wasted, while storage costs are not increased, showing the flexibility of the proposed solutions in case of unexpected disturbances, as well as the efficiency of the reactive strategy. An interesting observation can be made regarding the wasted doses, the large majority of which are Astrazeneca-type vaccines. Very few Pfizer-type and Johnson & Johnson-type vaccines are spoiled, while nearly no Moderna-type vaccines are wasted. The model correctly prioritizes the use of the costly mRNA vaccines, although very few Pfizer-type vaccines are lost due to their limited shelf-life and choses to waste the least expensive alternative (Astrazeneca-type vaccines). Detailed information on the wasted doses per iteration are given in Table S19 of the supplementary material.

5. Conclusions

In this work, the optimal planning of the COVID-19 VSC is considered. Specific problem characteristics, such as special cold storage requirements, extremely limited shelf-life of some vaccine types in refrigerated conditions and the unprecedented time pressure for the realization of the vaccination program, differentiates it from other similar supply chain problems. To the best of our knowledge, this is the first work to address the planning problem of the COVID-19 vaccine distribution chain. In addition, we extend this study by integrating decisions on optimally planning the daily vaccination program in every vaccination centre. A novel MILP model is developed to tackle this integrated problem. The model's efficiency is first shown in an illustrative example. Optimal decisions leading to the minimization of cost are generated in very low CPU times. Furthermore, a decomposition strategy extends the applicability of the model on realistically sized problems. A simulated instance of the Greek COVID-19 VSC is used to illustrate the capabilities of the proposed framework. Decisions on transferred quantities, inventory profiles, transportation, and staff requirements, as well as, daily vaccination plans, for a nationwide problem, are optimally taken in low CPU times. Finally, a reactive approach that utilizes a rolling horizon algorithm is proposed to handle uncertainties related to unexpected disturbances in the daily vaccination plan of the vaccination centres. Possible future research directions could be the consideration of more sophisticated clustering methods and the inclusion of vehicle routing decisions, through a metaheuristic, e.g. Variable Neighbourhood Search, approach.

CRediT authorship contribution statement

Georgios P. Georgiadis: Conceptualization, Methodology, Software, Investigation, Visualization, Writing – original draft. **Michael C. Georgiadis:** Conceptualization, Supervision, Writing - review & editing.

Declaration of Competing Interest

The authors declare that they have no known competing financial interests or personal relationships that could have appeared to influence the work reported in this paper.

Appendix A. Supplementary material

Supplementary data to this article can be found online at https://doi.org/10.1016/j.vaccine.2021.07.068.

References

[1] Lee BY, Haidari LA. The importance of vaccine supply chains to everyone in the vaccine world. Vaccine 2017;35(35):4475–9.
[2] Papageorgiou LG, Rotstein GE, Shah N. Strategic supply chain optimization for the pharmaceutical industries. Ind. Eng. Chem. Res. 2001;40(1):275–86.
[3] Gatica G, Papageorgiou LG, Shah N. Capacity planning under uncertainty for the pharmaceutical industry. Chem. Eng. Res. Des. 2003;81(6):665–78.
[4] Shah N. Pharmaceutical supply chains: key issues and strategies for optimisation. Comput. Chem. Eng. 2004;28(6-7):929–41.
[5] Amaro ACS, Barbosa-Povoa APFD. Planning and scheduling of industrial supply chains with reverse flows: a real pharmaceutical case study. Comput. Chem. Eng. 2008;32:2606–25.
[6] Masoumi AH, Yu M, Nagurney A. A supply chain generalized network oligopoly model for pharmaceuticals under brand differentiation and perishability. Transp. Res. Part E Logist. Transp. Rev. 2012;48(4):762–80.
[7] Weraikat D, Zanjani MK, Lehoux N. Coordinating a green reverse supply chain in pharmaceutical sector by negotiation. Comput. Ind. Eng. 2016;93:67–77.
[8] Sarkis M, Bernardi A, Shah N, Papathanasiou MM. Emerging challenges and opportunities in pharmaceutical manufacturing and distribution. Processes 2021;9(3):457.
[9] Liu R, Xie X, Garaix T. Hybridization of tabu search with feasible and infeasible local searches for periodic home health care logistics. Omega 2014;47:17–32.
[10] Kramer R, Cordeau J-F, Iori M. Rich vehicle routing with auxiliary depots and anticipated deliveries: an application to pharmaceutical distribution. Transp. Res. Part E Logist. Transp. Rev. 2019;129:162–74.
[11] Zahiri B, Zhuang J, Mohammadi M. Toward an integrated sustainable-resilient supply chain: a pharmaceutical case study. Transp. Res. Part E Logist. Transp. Rev. 2017;103:109–42.
[12] Savadkoohi E, Mousazadeh M, Torabi SA. A possibilistic location-inventory model for multi-period perishable pharmaceutical supply chain network design. Chem. Eng. Res. Des. 2018;138:490–505.
[13] Jankauskas K, Papageorgiou LG, Farid SS. Fast genetic algorithm approaches to solving discrete-time mixed integer linear programming problems of capacity planning and scheduling of biopharmaceutical manufacture. Comput. Chem. Eng. 2019;121:212–23.
[14] Wang X, Kong Q, Papathanasiou MM, Shah N. Precision healthcare supply chain design through multi-objective stochastic programming. Computer Aided Chemical Engineering, vol. 44. Elsevier; 2018. p. 2137–42.
[15] Papathanasiou MM, Stamatis C, Lakelin M, Farid S, Titchener-Hooker N, Shah N. Autologous CAR T-cell therapies supply chain: challenges and opportunities? Cancer Gene Ther. 2020;27(10-11):799–809.
[16] Karakostas P, Panoskaltsis N, Mantalaris A, Georgiadis MC. Optimization of CAR T-cell therapies supply chains. Comput. Chem. Eng. 2020;139:106913.
[17] Lee BY et al. The impact of making vaccines thermostable in Niger's vaccine supply chain. Vaccine 2012;30(38):5637–43.

[18] Zaffran M, Vandelaer J, Kristensen D, Melgaard B, Yadav P, Antwi-Agyei KO, et al. The imperative for stronger vaccine supply and logistics systems. Vaccine 2013;31:B73–80.
[19] Yadav P, Lydon P, Oswald J, Dicko M, Zaffran M. Integration of vaccine supply chains with other health commodity supply chains: a framework for decision making. Vaccine 2014;32(50):6725–32.
[20] Assi T-M et al. Removing the regional level from the Niger vaccine supply chain. Vaccine 2013;31(26):2828–34.
[21] Brown ST et al. The benefits of redesigning Benin's vaccine supply chain. Vaccine 2014;32(32):4097–103.
[22] Lee BY et al. Re-designing the Mozambique vaccine supply chain to improve access to vaccines. Vaccine 2016;34(41):4998–5004.
[23] Lemmens S, Decouttere C, Vandaele N, Bernuzzi M. A review of integrated supply chain network design models: Key issues for vaccine supply chains. Chem. Eng. Res. Des. 2016;109:366–84.
[24] Duijzer LE, van Jaarsveld W, Dekker R. Literature review: the vaccine supply chain. Eur. J. Oper. Res. 2018;268(1):174–92.
[25] Mula J, Peidro D, Díaz-Madroñero M, Vicens E. Mathematical programming models for supply chain production and transport planning. Eur. J. Oper. Res. 2010;204(3):377–90.
[26] Liu S, Papageorgiou LG. Multiobjective optimisation of production, distribution and capacity planning of global supply chains in the process industry. Omega (United Kingdom) 2013;41(2):369–82.
[27] Ramos TRP, Gomes MI, Barbosa-Póvoa AP. Planning a sustainable reverse logistics system: Balancing costs with environmental and social concerns. Omega 2014;48:60–74.
[28] Chen S, et al. A planning model for the WHO-EPI vaccine distribution network in developing countries A planning model for the WHO-EPI vaccine distribution network in developing countries. 2014:8830.
[29] de Carvalho MI, Ribeiro D, Barbosa-Povoa AP. Design and planning of sustainable vaccine supply chain. In: Barbosa-Povoa AP, Jenzer H, de Miranda JL, editors. Pharmaceutical Supply Chains - Medicines Shortages. Cham: Springer International Publishing; 2019. p. 23–55.
[30] Yang Y. Optimal design and operation of WHO-EPI vaccine distribution chains. 2017;1.
[31] Kontoravdi C, Shattock R, Shah N. Resources, production scales and time required for producing RNA vaccines for the global pandemic demand. 2021:1–14.
[32] Rastegar M, Tavana M, Meraj A, Mina H. An inventory-location optimization model for equitable influenza vaccine distribution in developing countries during the COVID-19 pandemic. Vaccine 2021;39(3):495–504.
[33] World Health Organization. Revising global indicative wastage rates: a WHO initiative for better planning and forecasting of vaccine supply needs. 2019.
[34] Brooke A, Kendrik D, Meeraus A, Raman R, Rosenthal RE. GAMS-A User's Guide. Washington, DC: GAMS Development Corporation; 1998.
[35] Hellenic Statistical Authority. 2011 Population-Housing Census; 2011.